Journal of Experimental & Clinical Cancer Research

RESEARCH

Open Access

Wild-type IDH1 inhibition enhances chemotherapy response in melanoma

Mehrdad Zarei[1,2], Omid Hajihassani[1], Jonathan J. Hue[2], Hallie J. Graor[1], Alexander W. Loftus[2], Moeez Rathore[1], Ali Vaziri-Gohar[1], John M. Asara[3,4], Jordan M. Winter[1,2*] and Luke D. Rothermel[1,2*]

Abstract

Background: Alternative treatment strategies in melanoma beyond immunotherapy and mutation-targeted therapy are urgently needed. Wild-type isocitrate dehydrogenase 1 (wtIDH1) has recently been implicated as a metabolic dependency in cancer. The enzyme protects cancer cells under metabolic stress, including nutrient limited conditions in the tumor microenvironment. Specifically, IDH1 generates NADPH to maintain redox homeostasis and produces α-ketoglutarate to support mitochondrial function through anaplerosis. Herein, the role of wtIDH1 in melanoma is further explored.

Methods: The expression of wtIDH1 was determined by qRT-PCR, and Western blot in melanoma cell lines and the effect of wtIDH1 on metabolic reprogramming in melanoma was interrogated by LC-MS. The impact of wtIDH1 inhibition alone and in combination with chemotherapy was determined in cell culture and mouse melanoma models.

Results: Melanoma patients express higher levels of the wtIDH1 enzyme compared to normal skin tissue, and elevated wtIDH1 expression portends poor patient survival. Knockdown of IDH1 by RNA interference inhibited cell proliferation and migration under low nutrient levels. Suppression of IDH1 expression in melanoma also decreased NADPH and glutathione levels, resulting in increased reactive oxygen species. An FDA-approved inhibitor of mutant IDH1, ivosidenib (AG-120), exhibited potent anti-wtIDH1 properties under low magnesium and nutrient levels, reflective of the tumor microenvironment *in natura*. Thus, similar findings were replicated in murine models of melanoma. In light of the impact of wtIDH1 inhibition on oxidative stress, enzyme blockade was synergistic with conventional anti-melanoma chemotherapy in pre-clinical models.

Conclusions: These results demonstrate the clinical potential of wtIDH1 inhibition as a novel and readily available combination treatment strategy for patients with advanced and refractory melanoma.

Keywords: Melanoma, IDH1, Ivosidenib, Chemoresistance, Combination therapy

*Correspondence: Jordan.Winter@UHHospitals.org; Luke.Rothermel@UHHospitals.org

[2] Department of Surgery, Division of Surgical Oncology, University Hospitals Cleveland Medical Center, 11100 Euclid Ave., Cleveland, OH 44106, USA
Full list of author information is available at the end of the article

Graphical Abstract

Schematic shows increased wild-type IDH1 expression and activity as an adaptive response to metabolic stress induced by chemotherapy.

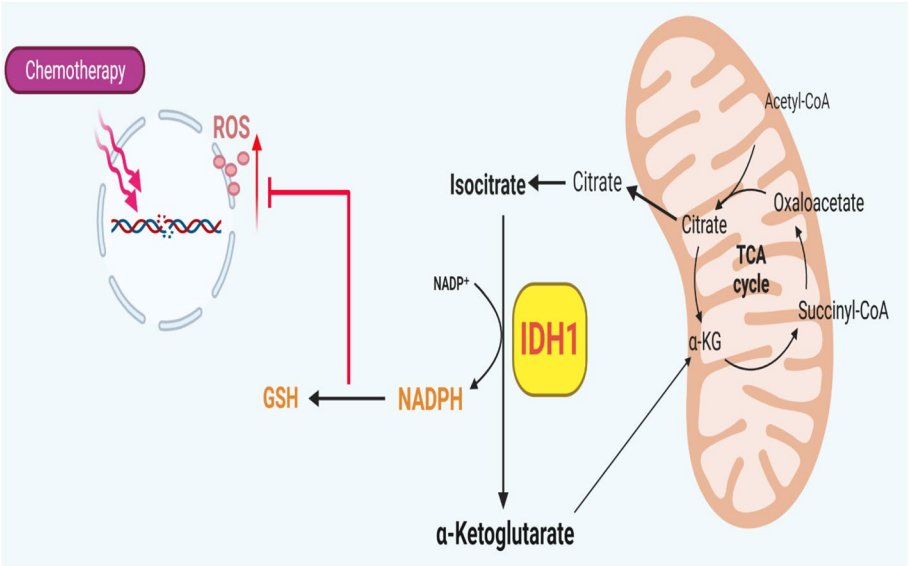

Background

Due to the availability of more effective therapeutics for advanced melanoma in the modern treatment era, chemotherapies are reserved for unique treatment scenarios [1, 2]. The five-year survival rate among patients with metastatic melanoma receiving combination immunotherapy with nivolumab and ipilimumab is over 50%, as compared to just 5% prior to the adoption of these therapies [3–5]. Despite clear progress, 40% of patients treated with dual checkpoint inhibitor therapy do not experience any response, and 60% of patients experience significant toxicities from therapy. In addition, over one-third of responders (20% overall) eventually develop secondary or acquired resistance [6–8]. Targeted therapies, such as BRAF and MEK inhibitors, have demonstrated success in patients with BRAF mutated tumors. However, only half of melanoma patients carry this mutation [9]. In such patients, the overall survival benefits of these targeted therapies are modest, and acquired resistance occurs for almost all patients during the first year of treatment [10]. Thus, while novel therapies have legitimately improved survival for patients with advanced melanoma, innate and acquired treatment resistance limits their generalizability and effectiveness. Attention in the field has concentrated heavily on these two areas of focus over the past decade (immunotherapy and oncogene-targeted therapy) at the expense of investigating alternative strategies to exploit critical biologic dependencies.

Prior to the use of contemporary immunotherapy and targeted therapies, treatment options for advanced melanoma were largely restricted to conventional chemotherapeutics. Dacarbazine (DTIC), an FDA-approved agent in melanoma, produced an objective response rate of 13 to 20%, with a median survival rate of just 5 to 6 months for patients with stage IV disease [11]. A DTIC derivative, temozolomide (TMZ), was comparable with respect to efficacy, but carried advantages of oral delivery and the ability to penetrate the blood-brain barrier [12]. Both are prodrugs of the active alkylating agent 5-(3-methyltriazen-1-yl) imidazole-4-carboxamide (MTIC) that induces apoptosis through direct DNA damage [13]. While these treatments have been deprioritized for melanoma, new insights into metabolic reprogramming of melanoma cells in the context of the microenvironment uncovers strategies to enhance chemotherapeutic efficacy and offer patients yet another impactful treatment approach.

For instance, the harsh tumor microenvironment in melanoma is characterized by hypoxia, tissue necrosis, and nutrient limitation [14–17]. Among other biologic processes, cancer cells rely on robust antioxidant defense to neutralize reactive oxygen species attributable to nutrient scarcity, as well as enhanced mitochondria function to maximize ATP production [18, 19]. Recently,

our group identified wild-type isocitrate dehydrogenase 1 (wtIDH1) as a key metabolic enzyme for both of these pro-survival cellular activities in pancreatic cancer [20]. Mechanistically, we showed that when cancer cells experienced nutrient withdrawal, the RNA binding protein Hu antigen R/ELAV like RNA-binding protein 1 (HuR), positively regulates wild-type IDH1, to increases antioxidant defense and overcome these harsh conditions. IDH1 is cytosolic and isofunctional to the mitochondrial enzymes IDH2 and IDH3A. The enzyme catalyzes the interconversion of isocitrate and alpha-ketoglutarate (αKG) using NADP(H) as a cofactor [21–23]. Under nutrient limitation, commonly present in tumors such as melanoma, oxidative decarboxylation of isocitrate is favored, producing NADPH and αKG. These products directly support antioxidant defense (NADPH is the reductive currency in cells) and mitochondrial function (αKG fuels the TCA cycle through anaplerosis), respectively [24].

Our recent studies in pancreatic cancer identified for the first time that small molecules developed as selective mutant-IDH1 inhibitors [25–28], actually inhibit wtIDH1 with a high degree of potency under conditions present in the tumor microenvironment [24]. Specifically, reduced magnesium levels in tumors allow mutant-IDH1 inhibitors to bind to the wtIDH1 allosteric site with greater affinity [29]. In the presence of cancer-associated stress (e.g., nutrient limitation), cancer cells are highly dependent on wtIDH1, rendering wtIDH1 inhibition with allosteric IDH1 inhibitors lethal to treated cancer cells.

Previous work demonstrates that the induction of high levels of oxidative stress in melanoma cells can be exploited to overcome chemotherapy resistance, since antioxidant capabilities become overwhelmed [30]. This paper is the first since our publication on pancreatic cancer [24] to validate the effectiveness of IDH1 inhibition in another cancer type. We build on upon this work to show that wtIDH1 is especially important for melanoma cell survival, and in particular, chemotherapy resistance. If true, this work provides a strong rationale to translate findings to clinical trials that test the combination of available wtIDH1 inhibitors with conventional chemotherapeutics largely abandoned for patients with advanced melanoma (e.g., DTIC or TMZ).

Materials and methods

Cell lines and cell culture

A375 (human), SK-MEL-28 (human), and B16-F10 (murine) melanoma cell lines were obtained from ATCC (American Type Culture Collection). Cells were cultured in DMEM supplemented with 10% FBS (Gibco/Invitrogen), and 1% penicillin-streptomycin (Invitrogen) at 37 °C in 5% humidified CO_2 incubators. Glucose-free DMEM (Life Technologies, 21013-024) was utilized for experiments with varying glucose concentrations, and the appropriate amounts of glucose were added to the media. For experiments with varied magnesium levels, magnesium sulfate-depleted DMEM (Cell Culture Technologies, 964DME-0619) was utilized, and supplemented with the indicated amounts of MgSO4. Cell lines were treated with prophylactic doses of Plasmocin and Mycoplasma tested (# MP0035, Sigma Aldrich) monthly. Cell lines were passaged at least twice before experimental use.

CRISPR construct knockout IDH1 in melanoma cells

CRISPR/Cas9-mediated knockout of *IDH1* was performed in A375, and SK-MEL-28 cells using guide RNAs targeting *IDH1* (GTAGATCCAATTCCACGTAGGG) fused with CRISPR/Cas9 and GFP protein. CRISPR Universal Negative Control plasmid (CRISPR06-1EA) was purchased from Sigma-Aldrich (St. Louis, MO). Cells were collected after 48 hours of transfection, and GFP-positive cells were single-sorted using FACS ARIA flow cytometer.

siRNA transfections

Cells were plated at 60% confluence in 6-well plates, and transient siRNA transfections (1 μM) were performed using Lipofectamine 2000 (Invitrogen) and Opti-MEM (Invitrogen) according to the manufacturer's protocol. Experiments were generally started 48 hours after transfections. Small interfering RNA (siRNA) oligos were purchased from Ambion (si*IDH1*, S7121; siCTRL, AM4635).

Cell viability assays

Cells were seeded in 96-well plates with 1×10^3 cells per well. After settling for 24 hours, cells were treated as indicated. Experiments lasted for 6 days unless otherwise detailed, and cell proliferation was estimated by staining with Quant-iT PicoGreen™ (Invitrogen). To estimate cell death, cells were trypsinized, stained with 0.4% Trypan blue (Invitrogen) after 0 to 4 days, and counted using a Hausser Scientific bright-line hemocytometer (Fisher Scientific).

Drug combination assays were performed after seeding 1-2 $\times 10^3$ cells per well in 96-well plates for 24 hours. Cells were treated with AG-120 (a wtIDH1 inhibitor, dose range: 0.125 μmol/ml - 2 μmol/ml) and TMZ (dose range: 6.25 μmol/ml - 800 μmol/ml) in a 6 X 8 well matrix, and experiments were repeated in triplicate. Cell viability was estimated after 6 days (compared to vehicle) with Quant-iT PicoGreen. Drug interactions were quantified and characterized as synergistic, additive, or antagonistic using the Bliss Independence model, as described [31]. For all in vitro experiments using AG-120, cells were

cultured under low magnesium conditions (< 0.4 mM Mg^{2+}) to effectively inhibit wtIDH1 enzyme activity (as a reference, normal culture media and serum contain roughly 1 mM Mg^{2+}). Low glucose (2.5 mM glucose) was utilized as indicated to generate conditions of wtIDH1 dependency and simulate glucose levels in the tumor microenvironment [32–36].

Immunoblotting

Cells were lysed using 1X RIPA buffer containing protease and phosphatase inhibitors. Protein concentration was quantified using the BCA Protein Assay (Thermo Fischer Scientific). Equal amounts of total protein were added to a 4–12% Bis-Tris gel (Life Technologies), separated by size using electrophoresis, and transferred to a PVDF membrane. Blots were blocked in 5% skimmed milk and probed with primary antibodies against IDH1 (Invitrogen, OTI2H9) and α-tubulin (Invitrogen, 11,224-1-AP). Chemiluminescent (32,106, Thermo Fisher Scientific) signal was captured using a digital imager (Odyssey Imaging system).

DNA sequencing

DNA was extracted from 1×10^6 human and murine melanoma cells using DNeasy Blood and Tissue kit (Qiagen) following the manufacturer's protocol. A portion of IDH1 gene exon 4 containing Arg132 was amplified using set pairs of primers, against the human sequence: IDH1 F:5′-ACCAAATGGCACCATACGA-3; IDH1 R: 5′-TTC ATACCTTGCTTAATGGGTGT-3′, and for mouse: IDH1 F:5′-ATTCTGGGTGGCACTGTCTT-3′; IDH1R: 5′- CTCTCTTAAGGGTGTAGATGCC-3′. PCR was performed using a DNA thermal cycler, and the products were analyzed by agarose gel electrophoresis. PCR products were sequenced using one of the amplification primers.

Migration assay

Cells were plated at a density of 6×10^4 cells in the upper chamber of a 6.5-mm Transwell with 8.0 µm pore polycarbonate membrane inserts (Corning). One hundred microliters of serum-free DMEM was added to the Transwells for 8 hours at 37 °C. Complete growth medium was placed in the bottom section as a chemoattractant. Non-migrated cells were wiped off the upper surface using cotton swabs. Cells migrating to the lower surface were fixed and stained using 0.5% crystal violet, imaged using a 10X objective on a Nikon TE200 microscope, and quantified using Image J analysis software.

Clonogenic assay

Cells ($2\text{-}3 \times 10^3$ cells per well) were seeded in 6-well plates and treated with AG-120 (or vehicle) at the indicated concentration, and under low MgSO4 (0.08 mM) conditions. After 8 days, cells were washed with 1X PBS, fixed in 80% methanol, and stained with 0.03% (w/v) crystal violet for 10 minutes. The dye was extracted with 10% glacial acetic acid and absorbance was measured at 600 nm using a GloMax plate reader (Promega) [37].

Cellular ROS and 8-OHdG analysis

Cells were seeded in 96-well black plates and incubated in 100 µL phenol red free media containing 10 µM H2-DCFDA (Invitrogen) for 45 min, at 37 °C, in the dark. Fluorescence was measured using an excitation wavelength at 485 nm and emission wavelength at 535 nm on a GloMax plate reader. 8-hydroxy-2-deoxyguanosine (8-OHdG) was measured (Abcam, AB201734) per the manufacturer's instructions. For apoptosis, the caspase3/7 (Caspase-GloTM Promega G8090) level was measured per the manufacturer's instructions.

Animal studies

All experiments involving mice were approved by the CWRU Institutional Animal Care Regulations and Use Committee (IACUC, protocol 2018-0063). Six-week-old female athymic nude mice (Nude-Foxn1nu) were purchased from Harlan Laboratories (6903M). A375 cells, or genetically modified variants, were suspended in 150 µL solution comprised of 60% Dulbecco's PBS and 40% Matrigel. Suspensions of 1×10^6 cells were injected subcutaneously into the right flank of mice. For syngeneic orthotopic experiments, 5×10^4 B16-F10 cells were suspended in the same manner and injected into flanks of immunocompetent 10 week-old C57BL/6J mice.

Treatments were initiated after tumors were first palpable and reached 100-120 mm^3 (nude mice) or 80-100 mm3

(See figure on next page.)

Fig. 1 Wild-type IDH1 is overexpressed in primary and metastatic melanoma. **A** RNA- sequencing data showing expression of *IDH1* in human primary melanoma compared to that in normal skin tissues, **P* < 0.05. **B** *IDH1* RNA expression in human primary melanoma compared to metastatic melanoma **P* < 0.05. **C** Correlation between IDH1 expression and overall survival rate of melanoma patients by Kaplan-Meier analysis using the log-rank test *P* < 0.035. The data of **A**, **B**, and **C** were obtained from the TCGA database. **D** *IDH1* mRNA expression level in different melanoma cell lines by qPCR. Expression levels are normalized to 18S expression in each cell line. **E** Representative immunoblot analysis of IDH1 in different melanoma cell lines and primary human melanocytes; alpha-tubulin used for normalization of cellular protein. The relative protein level of IDH1 across three experiments is quantified by densitometry. Each data point represents the mean ± SEM of three independent experiments. *, *P* < 0.05; **, *P* < 0.01; ***, *P* < 0.001)

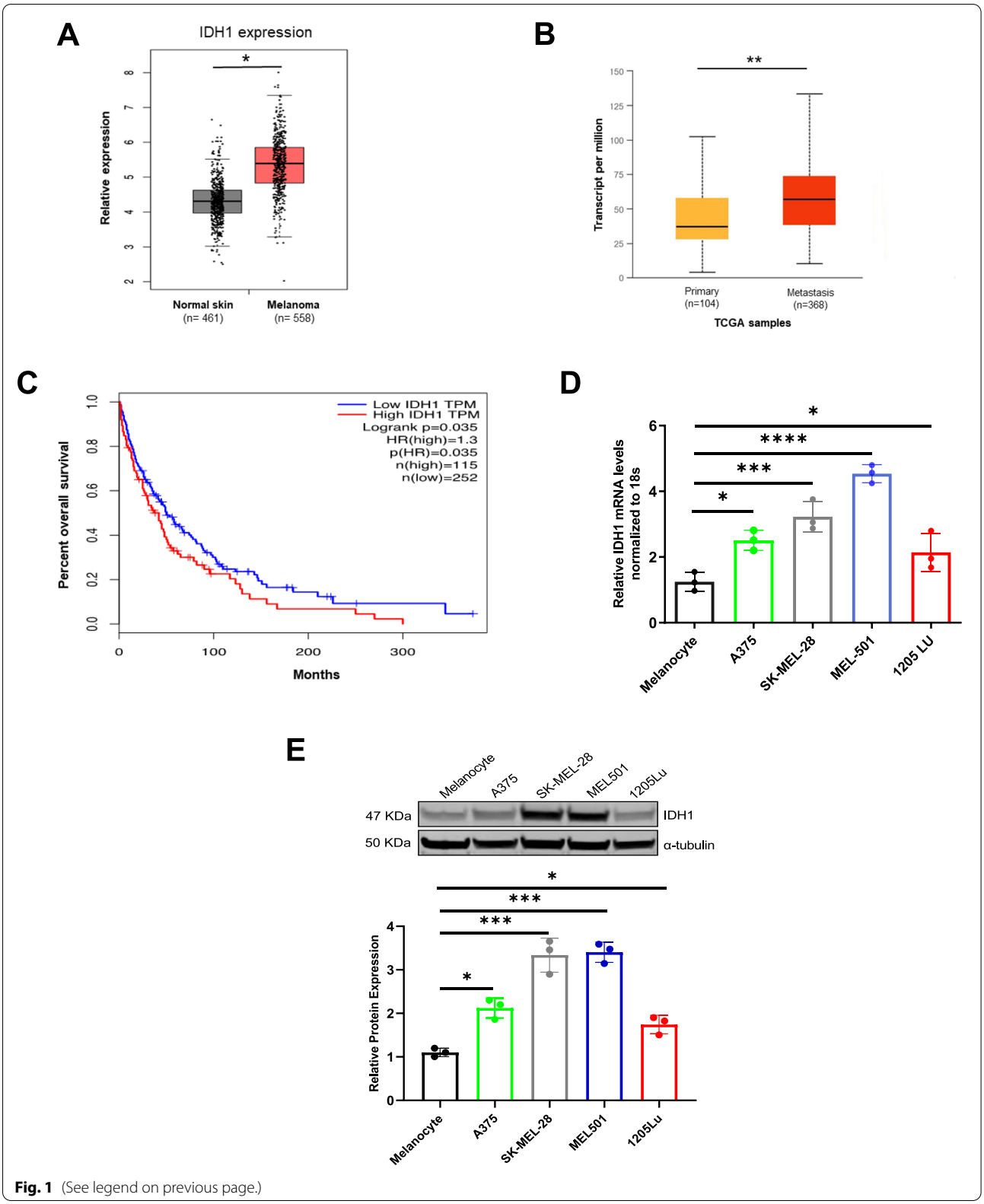

Fig. 1 (See legend on previous page.)

(C57BL/6J mice). AG-120 (Asta Tech, 40,817) was administered orally at 150 mg/kg twice per day as a suspension in PEG-400, Tween-80, and saline (10:4:86). TMZ (Sigma-Aldrich, T2577) was given at 30 mg/kg as intraperitoneal injections, five times per week. Bodyweights and tumor volumes were measured weekly. For the latter, Vernier calipers were utilized and volumes estimated by the formula, Volume = (Length × Width^2)/2. At the end of the experiment, mice were euthanized by carbon dioxide inhalation and tumors were immediately resected for additional studies. For immunohistochemistry analysis, tumors were fixed in 10% formalin (Thermo Fisher Scientific; 427-098) and stored at − 80 °C.

Real-time quantitative PCR

RNA was extracted using the RNeasy PureLink RNA isolation (Life Technologies; 12,183,025) and converted to cDNA using a High-Capacity cDNA Reverse Transcription Kit, per the manufacturer's protocol (Applied Biosystems; 4,387,406). qPCR was performed using Taqman™ Universal Master Mix II (Thermo Fisher Scientific; 4,440,038) with an IDH1 probe (Thermo Fisher Scientific; 4,351,372) and analyzed using the Bio-Rad CFX Maestro manager 2.0 software. Experiments are repeated in triplicate.

Metabolites extraction and measurement by LCMS

Cells were grown to ~ 50% confluence in complete growth medium in 6-well plates and in biological triplicates. After rinses with ice-cold PBS, metabolites were extracted with 80% HPLC-grade methanol, scraped, and collected. Polar metabolites were analyzed by 5500 QTRAP triple quadrupole mass spectrometry (AB/SCIEX) coupled to a Prominence UFLC HPLC system (Shimadzu) using amide HILIC chromatography (Waters) at pH 9.2, as previously described [38]. Two hundred ninety-nine endogenous water-soluble metabolites were measured at a steady state. Data were normalized to protein content. NADPH (NADP/NADPH-Glo™ Promega G9081) and glutathione (GSH) levels (GSH-Glo™ Promega V6911) were also measured separately per the manufacturer's instructions.

Bioenergetics

Oxygen consumption rates (OCR) and extracellular acidification rates (ECAR) were quantified using the XFp mini extracellular analyzer (Seahorse Bioscience). A375 cells were seeded at 1×10^4 cells per well in complete DMEM (25 mM glucose and 2 mM glutamine) in an Agilent XFp Cell Culture miniplate (#103025-100), and cultured at 37 °C in 5% humidified CO_2 incubators. For these experiments, glucose-free DMEM was supplemented with glucose to achieve the indicated concentrations, and incubated for an additional 36 hours. The XFp FluxPak cartridge (#103022-100), was hydrated and incubated at 37 °C, using non-CO_2 incubator overnight. The following day, cells were washed twice and replaced with Seahorse XF base media (using the indicated glucose concentrations), and incubated in a non-CO_2 incubator at 37 °C. OCR and ECAR were measured in the standard fashion using standard mitochondrial inhibitors: 1.5 µM oligomycin, 2 µM FCCP, and 0.5 µM rotenone + 0.5 µM antimycin A (Mito Stress Test, #103015-100). Data were normalized to cell number, as measured by Quant-iT PicoGreen™ (Invitrogen).

Magnesium and glucose measurements

Tissues were collected and homogenized in 10% sucrose on ice, followed by centrifugation at 12,000 rpm for 10 mins at 4 °C. Supernatants were collected and the free Mg^{2+} content was examined using atomic absorbance spectrometry (50 AA, Agilent Technologies). Results were normalized to homogenate weight and volume. Intera-tumoral glucose levels (Glucose-Glo™ Promega J6021) were measured per the manufacturer's instructions.

Statistical analysis

Major findings were replicated using a second cell line whenever possible. Data were expressed as mean ± SEM (standard error of the mean) of at least three independent experiments. Comparisons between groups were determined using an unpaired, two-tailed Student *t*-test (* $p < 0.05$; ** $p < 0.01$; *** $p < 0.001$ **** $p < 0.0001$). The one-way or two-way ANOVA test was used for comparisons

(See figure on next page.)

Fig. 2 IDH1 knockdown suppresses melanoma cell growth and induces ROS under glucose withdrawal. **A** Sanger sequencing of PCR amplicons correlated with codon 132 of the IDH1 gene in A375 and SK-MEL-28 cells. **B** qPCR and immunoblot analysis for IDH1 expression in A375 and SK-MEL-28 under 2.5 mM glucose compared with 25 mM glucose for 48 hours. **C** qPCR and immunoblot analysis for IDH1 expression after IDH1 silencing by siRNA oligos (si.IDH1) compared with control (si.CTRL) in A375 and SK-MEL-28 cells. **D** Relative ROS levels in si.CTRL and si.IDH1 A375 and SK-MEL-28 cells for 48 hours under the indicated glucose concentrations. **E** Schematic of the IDH1 enzymatic reaction. **F** Relative NADPH levels in A375 and SK-MEL-28 cells cultured under the indicated conditions for 72 hours. **G** Relative GSH levels in si.IDH1 and si.CTRL A375 and SK-MEL-28 cells under the indicated glucose concentration. **H** Relative 8-OHdG levels in DNA extracted from A375 and SK-MEL-28 cells under indicated conditions for 48 hours. **I** Cell viability (trypan blue assays) of A375 and SK-MEL-28 after silencing IDH1 compared to control (si.CTRL) under high and low glucose conditions for the indicated time points. Each data point represents the mean ± SEM of three independent experiments. N.S., nonsignificant; *, $P < 0.05$; **, $P < 0.01$; ***, $P < 0.001$; ****, $P < 0.0001$

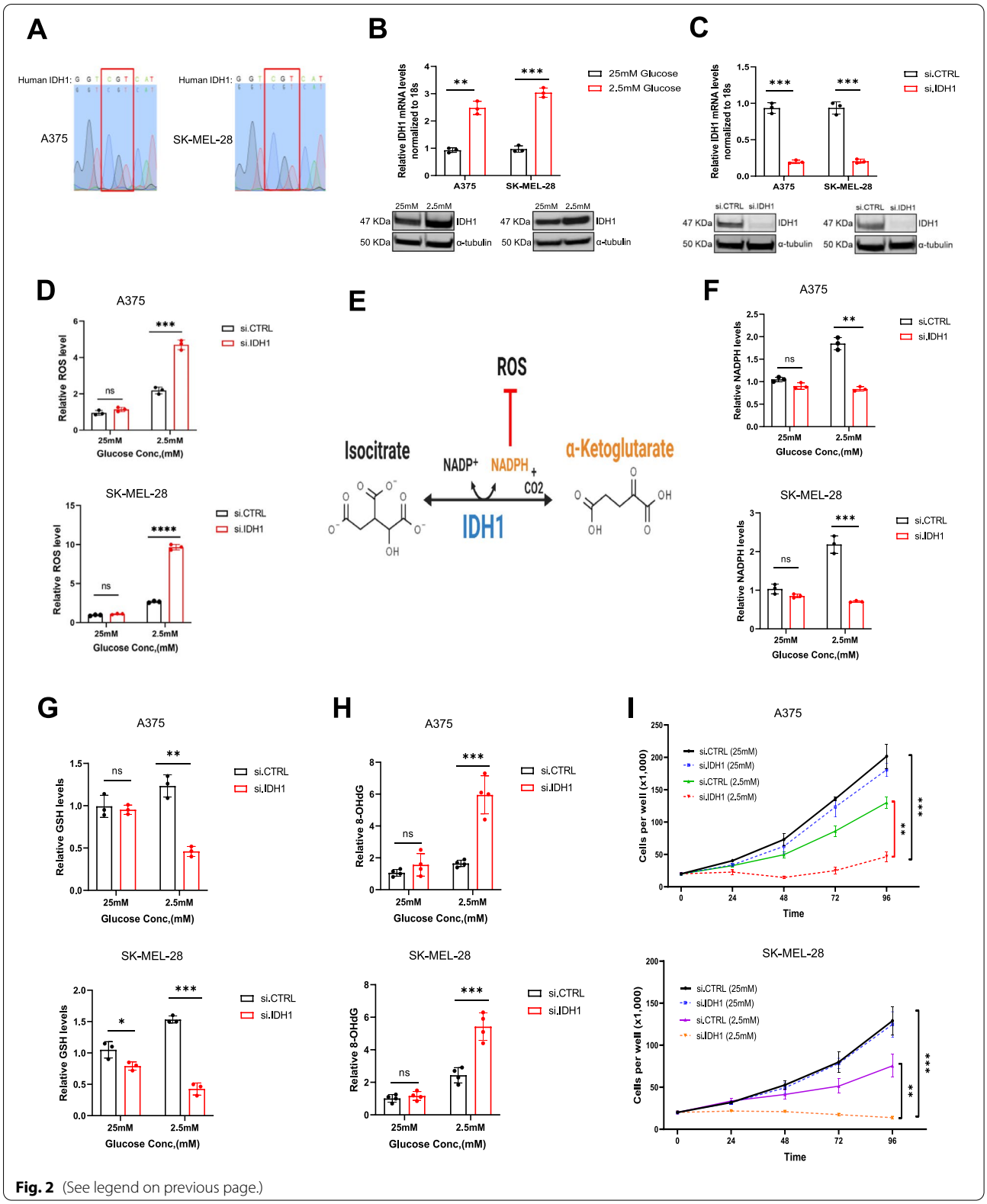

Fig. 2 (See legend on previous page.)

between more than two groups. GraphPad Prism 9.2.3 software was used for statistical analyses.

Results

Increased IDH1 expression in melanoma

Analysis of TCGA (The Cancer Genome Atlas) database revealed increased wt*IDH1* mRNA expression in tissues from primary and metastatic melanoma patients, as compared to normal skin. Kaplan-Meier analysis of IDH1 showed that higher mRNA expression of IDH1 in tumors is associated with poor overall survival in patients (Fig. 1A-C). Increased IDH1 expression was also observed at mRNA and protein levels in multiple human melanoma cell lines, as compared to normal melanocytes (Fig. 1D and E).

IDH1 impacts growth and antioxidant defense under nutrient withdrawal in melanoma cells

Human melanoma cells were first confirmed to contain wtIDH1 genomic sequence (Fig. 2A). Cells were subsequently cultured in normal tissue culture media (25 mM glucose, supra-physiologic) or low glucose conditions (2.5 mM). Acute glucose withdrawal led to an acute increase in IDH1 mRNA and protein expression in melanoma cells (Fig. 2B), likely as an adaptive metabolic response, previously observed in pancreatic cancer cells cultured under similar conditions [20]. IDH1 siRNA silencing (Fig. 2C) led to more than a two-fold increase in ROS levels under low glucose conditions. The effect was negligible under high glucose conditions, highlighting the expendability of the enzyme under nutrient abundance (Fig. 2D).

The impact of IDH1 on cancer cell antioxidant defense was likely attributable to enhanced generation of NADPH related to upregulated IDH1 expression (Fig. 2E) observed with low glucose stress (Fig. 2F). IDH1 silencing abrogated the increase in NADPH (Fig. 2F). Similarly, siRNA suppression of IDH1 diminished glutathione (GSH) levels under low glucose conditions, but lacked impact under glucose abundance (Fig. 2G). The high level of ROS lead to DNA damage, and 8-hydroxy-2-deoxyguanosine (8-OHdG) analyses revealed increased levels of DNA oxidation after siRNA suppression of *IDH1*, particularly under low glucose (Fig. 2H). Caspase 3 levels also increased with IDH1 silencing under glucose withdrawal (Supplementary Fig. S1A and B).

Cell proliferation studies mirrored these results. Under low glucose conditions, IDH1-deficient cells failed to proliferate, yet IDH1-deficient melanoma cell growth was unaffected under high glucose conditions (Fig. 2I). Along these lines, IDH1 expression similarly affected cell migration of melanoma cells, especially under low glucose conditions (Supplementary Fig. S1C and D).

Metabolic changes associated with IDH1 expression

Under glucose withdrawal, parental melanoma cells experience increased mitochondrial respiration (OCR) and reduced glycolysis (ECAR) (Supplementary Fig. S2A and B), underscoring the importance of mitochondrial metabolism under nutrient scarcity. Suppression of IDH1 blocked this adaptive reprogramming and enhanced oxidative stress. Liquid chromatography coupled tandem-mass-spectrometry (LC-MS/MS) metabolomics in melanoma cells cultured under low glucose conditions revealed distinct metabolomic profiles supporting this interpretation (Fig. 3A and Supplementary Fig. S2C). Hierarchical clustering and heatmap profiling of the top 50 altered metabolites (Fig. 3B and C) demonstrated reductions in mitochondrial TCA metabolites and associated metabolites of the TCA cycle (ATP and NADH), as well as a redox shift reflective of significant oxidative stress under low glucose (e.g., NADP+). Of note, the two products of IDH1 oxidative decarboxylation (αKG and NADPH) were both reduced with IDH1 suppression, and upstream reactants (citrate, isocitrate and NADP+) were increased (Fig. 3B and C). Pathway enrichment analysis confirmed TCA cycle suppression with IDH1 silencing, as well as dysregulation of other metabolic pathways, including pyrimidine synthesis and glutamine/glutamate metabolism (Fig. 3D). Some of these changes were apparent under high glucose but were less pronounced (Supplementary Fig. S2C, D). Consistent with these findings, siRNA against IDH1 under low glucose conditions substantially reduced OCR in melanoma cells (Fig. 3E and F), with negligible effects under high glucose conditions (Supplementary Fig. S2E).

(See figure on next page.)

Fig. 3 IDH1 supports mitochondrial function under stress. **A** Principal-component analysis (PCA) of metabolites analyzed by LC-MS/MS performed on A375 cells, after transfection with si.IDH1 and si.CTRL ($n = 3$ samples). **B** A heatmap of the top 50 metabolites with the greatest change in A375 cells after transfection with si.IDH1 versus si.CTRL ($n = 3$ independent samples) under 2.5 mM glucose and analyzed by LC/MS. The scale is log 2 fold-change. **C** Relative levels of TCA cycle metabolites from A375 after transfection with si.IDH1 and si.CTRL under 2.5 mM glucose for 12 hours. **D** Metabolite set enrichment analysis of A375 cells. **E** Representative oxygen consumption rate (OCR) in A375 cells transfected with si.IDH1 and si.CTRL, and cultured in 2.5 mM glucose for 24 hours. Treatment with mitochondrial inhibitors are indicated: oligomycin (Oligo), FCCP, antimycin A and rotenone (Anti/Rot) and **F** Basal mitochondrial OCR. Each data point represents the mean ± SEM of three independent experiments. N.S., nonsignificant; *, $P < 0.05$; **, $P < 0.01$; ***, $P < 0.001$

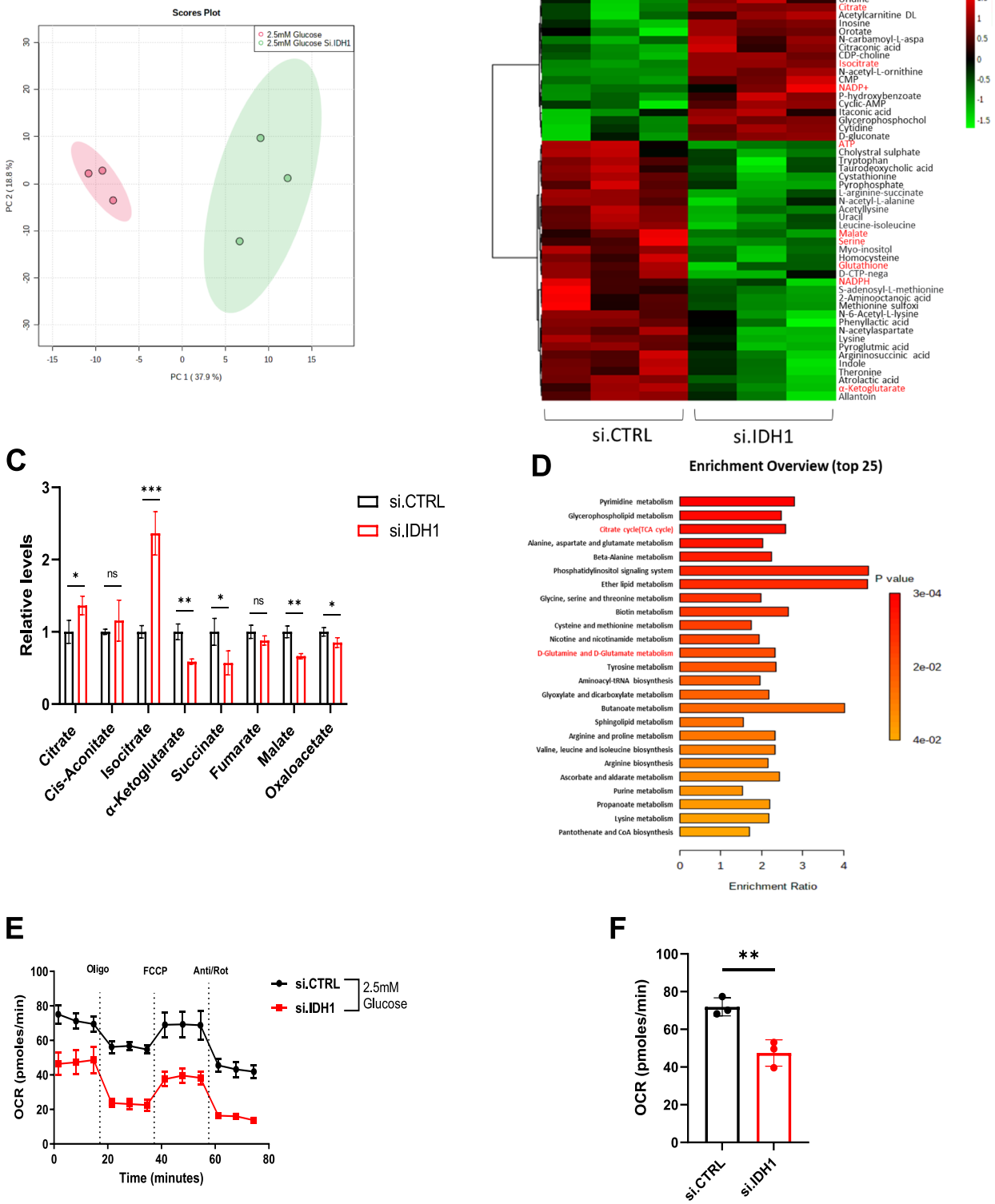

Fig. 3 (See legend on previous page.)

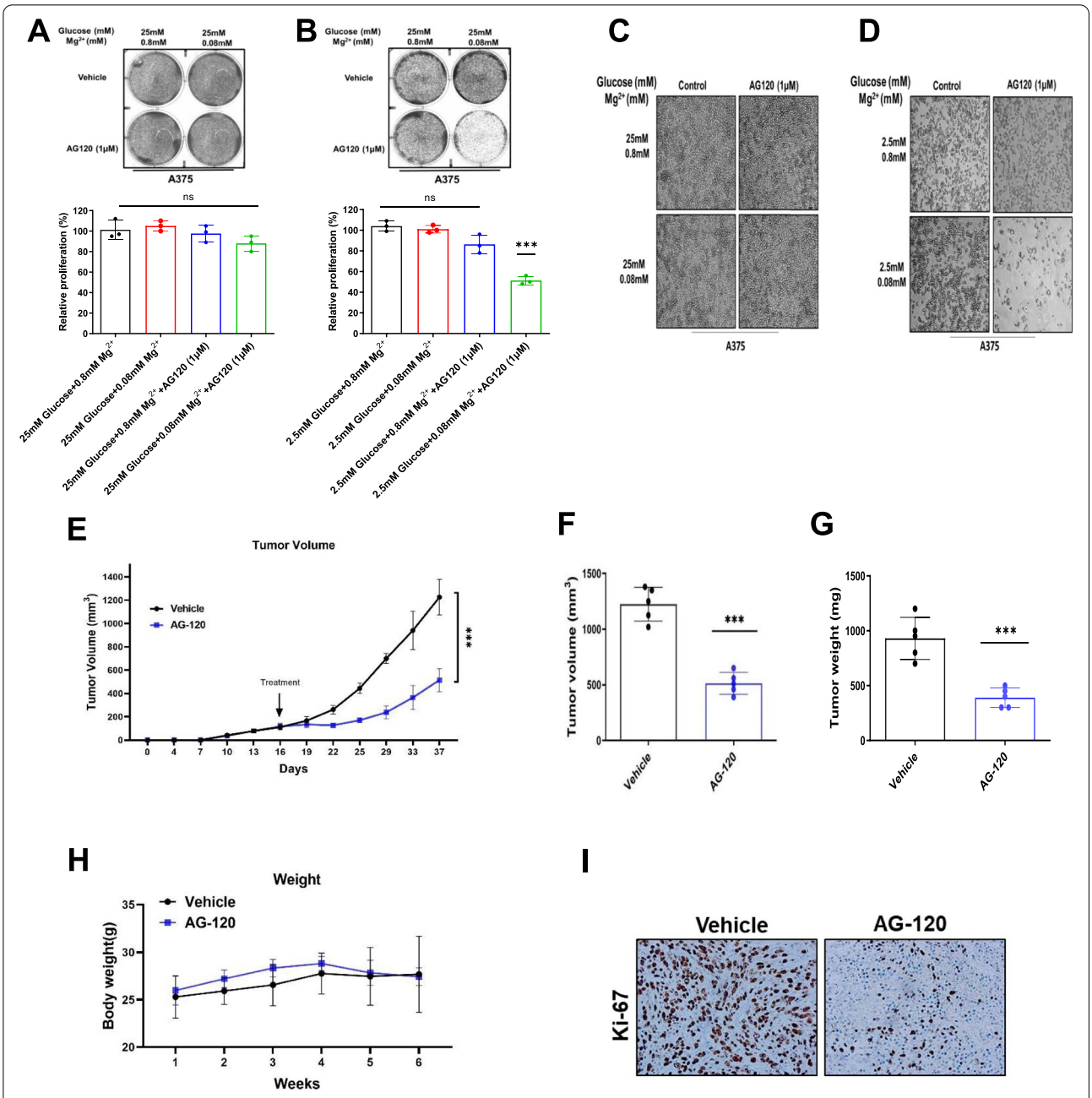

Fig. 4 AG-120 is a potent wild-type IDH1 inhibitor under low glucose and magnesium conditions. **A** Representative images of high glucose (25 mM) and **B** low glucose (2.5 mM) colony formation assays in the A375 cell line. Cells were treated with vehicle control and AG-120 (1 μM) under the indicated conditions, and stained with crystal violet solution. Quantification (%) is shown in the graphs. **C** Under high glucose and **D** low glucose conditions, phase-contrast images (4X magnification) were taken after treated with vehicle control or AG-120 (1 μM) for 4 days under indicated nutrient conditions. **E** Representative image of excised and in vivo tumors of A375. **F** Tumor growth curves of A375 melanoma xenografts in nude mice. Tumor sizes were assessed twice per week using calipers ($n = 5$ per group). **G** Average tumor volume of A375 xenografts at the end of the experiment (day 26) ($n = 5$ tumors per group). **H** Average tumors weights (mg) of A375 xenografts in each group ($n = 5$ per group). **I** Body weights of A375 melanoma xenografts in nude mice ($n = 5$ per group). **J** Cell mitoses in tumor xenografts were estimated by nuclear immunolabeling (Ki-67). Scale bar, 50 μm. Each data point represents the mean ± SEM of three independent experiments. N.S., nonsignificant; *, $P < 0.05$; **, $P < 0.01$; ***, $P < 0.001$; ****, $P < 0.0001$

Pharmacologic inhibition of IDH1 reduces cell viability and inhibits tumor progression

Ivosidenib (AG-120) is an FDA-approved drug developed to selectively target mutant IDH1 [39–41]. We recently discovered that the drug potently inhibits wtIDH1 under low Mg^{2+} conditions in pancreatic cancer models, as the cation competes with the inhibitor for negatively charged amino acid residues at the allosteric site [24]. Herein, we observed that AG-120 had minimal impact on melanoma survival in a clonogenic assay under high Mg^{2+} or high glucose conditions in two separate cell lines. However, under low Mg^{2+} and low glucose conditions, pharmacologic wtIDH1 inhibition paralleled the above results observed with IDH1 gene suppression. Treatment impaired melanoma survival at low glucose levels, since cells are dependent on wtIDH1 for antioxidant defense and mitochondrial function under this condition (Fig. 4A and B; Supplementary Fig. S3A and B). These results were recapitulated in an independent cell proliferation assay (Fig. 4C and D; Supplementary Fig. S3C and D). Further, to confirm the metabolic changes with AG-120, OCR was measured and showed that AG-120 phenocopied the metabolic changes of silencing IDH1 (Supplementary Fig. S3E and F). More specifically, we observed AG-120 significantly impaired the basal oxygen rate, decreased ATP production and decreased maximal mitochondrial respiration suggesting on-target pharmacologic action against wtIDH1 (Supplementary Fig. S3G and H).

IDH1 was subsequently deleted from melanoma cell lines using CRISPR/Cas9 editing (Supplementary Fig. S4A, IDH1-KO). Equal numbers of IDH1-KO and control cells were injected into the flanks of nude mice. Unlike control cells, IDH1-KO cells failed to grow well in vivo (Supplementary Fig. S4B-D). Findings were replicated with pharmacologic studies. AG-120 was administered at the same dose previously used in animal studies of mutant IDH1 tumors (150 mg/kg orally twice a day) [42, 43]. Treatment significantly impaired tumor growth without any appreciable weight loss in the mice (Fig. 4E-H). Notably, intra-tumoral glucose and Mg^{2+} levels were markedly reduced in this in vivo melanoma model compared to adjacent normal skin and serum (Supplementary Fig. S4E-F). Diminished cancer cell proliferation was validated by Ki-67 immunolabeling of harvested tumors (Fig. 4I).

Targeting IDH1 sensitizes melanoma cells to chemotherapy

TMZ is one of the two most commonly used chemotherapeutics (the other being DTIC) in patients with advanced melanoma. In prior clinical studies, TMZ achieved a dismal objective response rate of just 14% [44]. TMZ is known to exhibit oxidative and cytotoxic effects on melanoma [45] and IDH1 inhibition enhances both total cellular ROS and oxidative damage within the nucleus (Fig. 2D and H). Thus, we hypothesized that IDH1 inhibition would synergize with this melanoma associated-chemotherapy. We further hypothesized that the combination may be effective irrespective of glucose levels where chemotherapy agitates ROS under glucose abundance, similar to glucose limitation. In fact, IDH1 siRNA silencing resulted in a three- and nine-fold increase in TMZ sensitivity under high and low glucose conditions, respectively (Fig. 5A and B, Supplementary Fig. S5A and B).

Similar results were observed with pharmacologic IDH1 inhibition. Targeting IDH1 in combination with chemotherapy treatment under low glucose led to more than a three-fold increase in ROS levels, compared to chemotherapy alone (Supplementary Fig. S5C and D). Dose response data using each drug alone (Fig. 5C and D, Supplementary Fig. S5E and F) informed drug dosing in drug combination studies. Synergy experiments revealed that pharmacologic IDH1 inhibition rendered TMZ substantially more potent (up to 18-fold at some dosing levels) in melanoma cell lines, A375 and SK-MEL-28 (Fig. 5E and F, Supplementary Fig. S5G and H). For instance, TMZ alone had an IC50 of 155.89 µM against A375 cells, and this lack of potency is consistent with poor clinical efficacy. The addition of AG-120 at a dose slightly below the AG-120 IC50 concentration (1 µM) shifted the TMZ IC50 downward by more than an order of magnitude (to 8.4 µM). As a result, a positive Bliss score with various dosing combinations was observed.

IDH1 inhibition increases melanoma sensitivity to TMZ in vivo

Importantly, the combination of these drugs given to mice revealed enhanced anti-tumor activity in vivo.

(See figure on next page.)

Fig. 5 Targeting IDH1 sensitizes melanoma cells to conventional anti-melanoma cytotoxic therapy. **A** Silencing IDH1 followed by treatment with TMZ for 5 days under high glucose (25 mM) and **B** low glucose concentrations (2.5 mM) in the A375 cell line. IC_{50} values are provided. **C** Cell viability of the A375 cell line treated with the indicated doses of TMZ. IC_{50} values are provided. **D** Cell viability of the A375 cell line treated with indicated doses of AG-120. IC_{50} values are provided. **E** Drug sensitivity in the A375 cell line under low glucose concentrations and with varying doses of TMZ and AG-120 cultured for 5 days. IC_{50} is provided. **F** Drug matrix heatmap 5 × 8 (AG-120 and TMZ) grid showing percent viability and Bliss Independence scores in A375 cells cultured under 2.5 mM glucose for 5 days. Positive values reflect synergy and appear blue on the heatmap. All treatments with AG-120 were carried out under low glucose and low Mg^{2+} concentrations

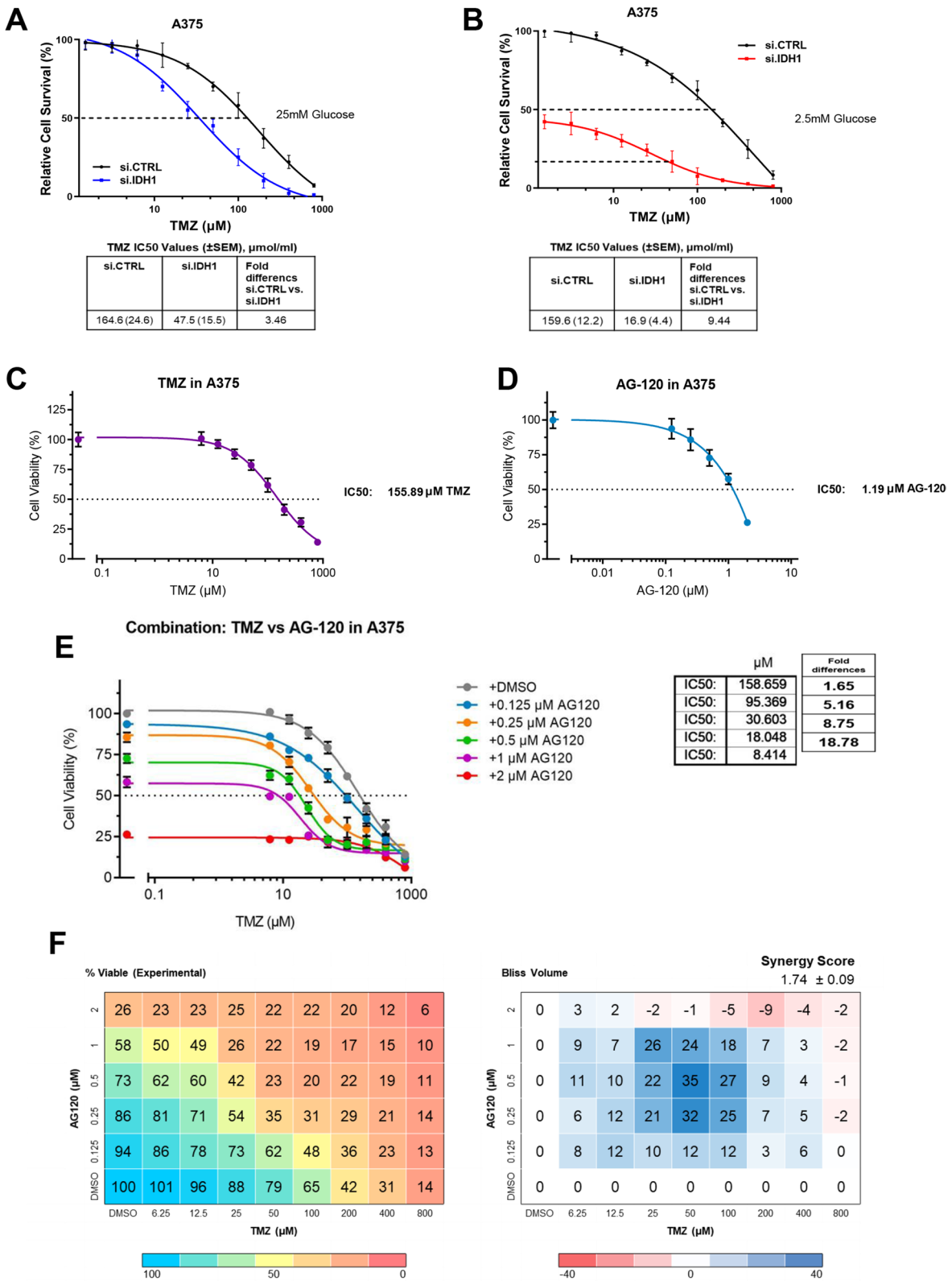

Fig. 5 (See legend on previous page.)

Two groups of mice were treated: Nude mice bearing human melanoma A375 cells (Fig. 6), and C57BL/6 J mice (Supplementary Fig. S6) with tumor derived from murine B16-F10 melanoma cells (containing the wtIDH1 genomic sequence (Supplementary Fig. S6A). Treatment arms included vehicle, TMZ (30 mg/kg intraperitoneal once a day), AG-120 (150 mg/kg orally twice a day), or combination AG-120 + TMZ (150 mg/kg orally twice a day + 30 mg/kg intraperitoneal daily) (Fig. 6A and Supplementary Fig. S6B). While AG-120 was more effective than conventional chemotherapy as a single-agent, the combination was by far the most effective, as evidenced by both a reduction in tumor growth (Fig. 6B-D) and improved mouse survival (Supplementary Fig. S6C). The drug combination was well-tolerated by mice, without any reduction in body weight (Fig. 6E). The effect of the combination was validated molecularly by a substantial reduction in Ki-67 immunolabeling in harvested tumors (Fig. 6F) and a dramatic increase in cleaved caspase-3 immunolabeling (Fig. 6G).

Discussion

Tumor cells grow in harsh metabolic microenvironments and require robust molecular strategies to combat oxidative stress for survival [14]. It follows then that cancer cell adaptations supporting the neutralization of reactive oxygen species would favor tumor growth. Consistent with this notion, multiple studies in mice and humans reveal that antioxidant supplementation increases tumor growth and promotes progression in diverse cancer types, including melanoma, due to a rescue effect [45–48]. This observation can be leveraged for therapeutic purposes. Targeting key components of antioxidant defense in tumors would conversely thwart cancer progression and metastasis by exacerbating the threat imposed by oxidative stress [49, 50].

We show here that wtIDH1 is a compelling therapeutic target in this regard because it is a metabolic vulnerability. Indeed, a small number of important studies previously cast a light on the enzyme as a promising therapeutic target in cancer. The pioneering work in this group of studies actually employed in vitro melanoma models but was never further pursued until the present work. Metallo et al. first observed that under hypoxic conditions, wtIDH1 activity was critical for melanoma cell survival because it encouraged the IDH1 reaction towards reductive metabolism (to the left in Fig. 2E) [23]. That is, in the absence of glucose withdrawal, αKG derived from glutamine was converted into isocitrate and propelled carbon substrate towards de novo lipogenesis and tumor growth. In that report, targeting IDH1 with siRNAs impaired cell proliferation under those conditions. Later, Jiang et al. showed that reductive carboxylation of glutamine was also important for anchorage-independence in tumor spheroids of different cancer types, and that this was again highly dependent on wtIDH1 [21]. Isotope tracer studies suggested that the cytosolic isocitrate produced by wtIDH1 through the reductive reaction was transferred to mitochondria, where oxidation back to αKG by mitochondrial IDH2 augmented NADPH and minimized mitochondrial ROS. Calvert et al. was the first to demonstrate that wtIDH1 favors oxidative decarboxylation (to the right in Fig. 2E) in certain tumor models (e.g., glioblastoma) to produce cytosolic NADPH for antioxidant defense and ROS control [51]. Targeting IDH1 augmented oxidative stress and reduced glioblastoma growth.

We recently validated the importance of wtIDH1 in diverse pancreatic cancer models, and established several key principals in that work. First, wtIDH1 was especially important for cancer cell survival under nutrient limiting conditions. Both NADPH and αKG produced by the oxidative decarboxylation of isocitrate (to the right in Fig. 2E) were critical for adaptive survival under these conditions. Second, both oxidative IDH1 reaction products mechanistically support mitochondrial function, in addition to antioxidant defense. This wtIDH1 function was also essential for cancer cell survival under metabolic stress in cell culture and in mouse cancer models. αKG serves a key anaplerotic role in support of TCA cycling and mitochondrial function, while NADPH reduces mitochondrial ROS. Third, AG-120 and other allosteric wtIDH1 inhibitors developed to selectively target the

(See figure on next page.)

Fig. 6 Treatment of mice bearing melanoma xenografts with TMZ in combination with AG-120. **A** Schematic represents the treatment model after 1×10^6 A375 melanoma cells were injected subcutaneously into the flank of nude mice. A separate experiment with B16-F10 melanoma murine cells involved 4×10^4 cells injected subcutaneously into C57BL/6 J recipient mice. After 8-10 days, when tumors reached 100-120 mm^3, mice were divided into four groups and treated with i) Vehicle; ii) TMZ (30 mg/kg) every day; iii) AG-120 (150 mg/kg) twice a day; iv) AG-120 + TMZ (150 mg/kg + 30 mg/kg). **B** Tumor growth curves of A375 melanoma xenografts in nude mice. Tumor sizes were assessed twice per week using calipers ($n = 5$ per group), **C** Average tumors weights (mg) of A375 xenografts in each group ($n = 5$ per group). **D** Representative image of excised and in vivo tumors of A375. **E** Body weights of A375 melanoma xenografts in nude mice ($n = 5$ per group). **F** Cell proliferation in tumor xenografts was estimated by nuclear immunolabeling (Ki-67). Scale bar, 50 µm. Quantitation is shown below from four random fields per section. **G** Tumor xenograft apoptosis was estimated with labeled cleaved caspase-3. Quantitation is shown below from four random fields per section. Scale bar, 50 µm. Each data point represents the mean ± SEM of at least three independent experiments. *, $P < 0.05$; **, $P < 0.01$; ***, $P < 0.001$; ****, $P < 0.0001$

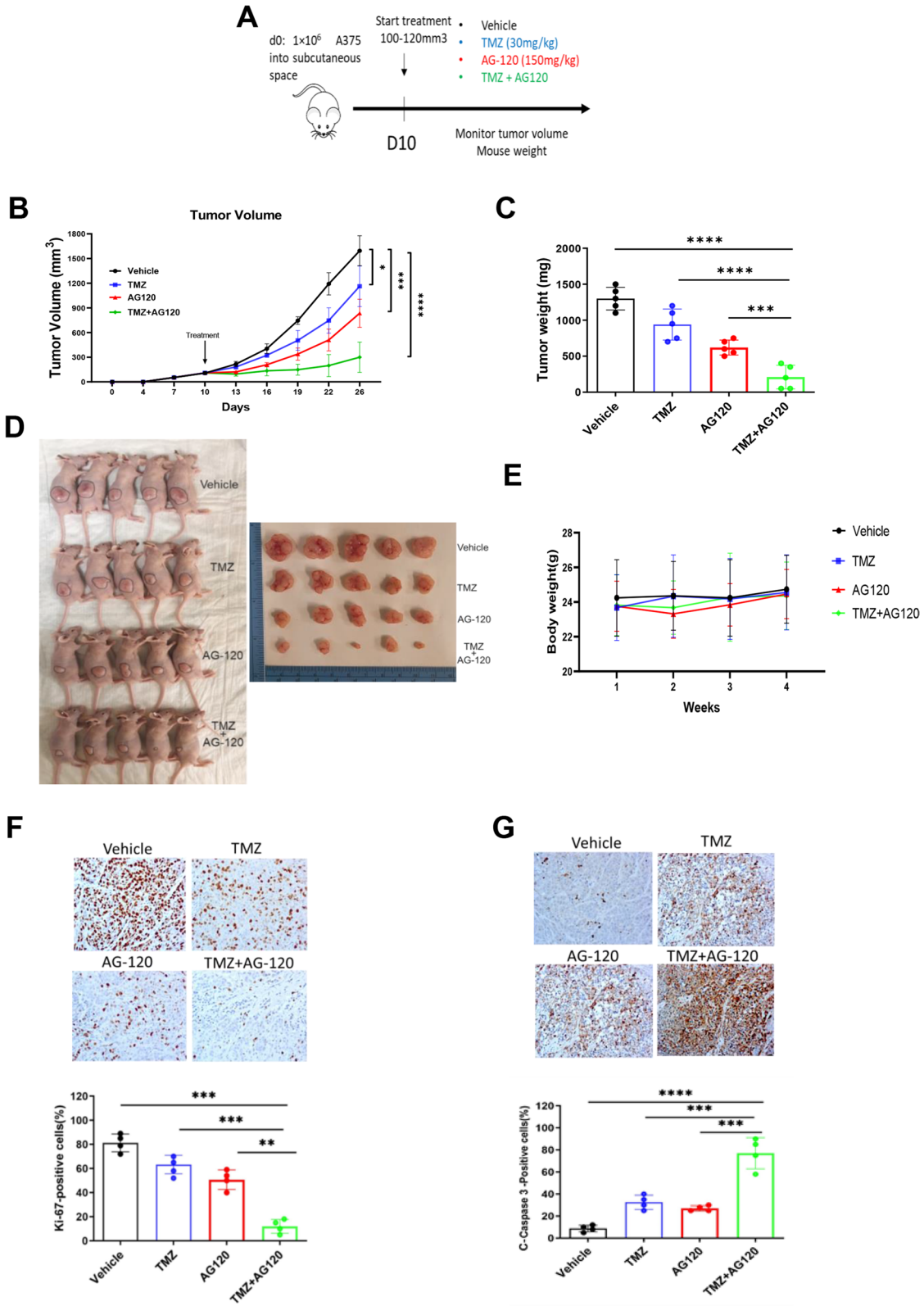

Fig. 6 (See legend on previous page.)

mutant IDH1 isoenzyme, are actually potent wtIDH1 inhibitors in tumors due to two specific conditions present to the tumor microenvironment: low Mg^{2+} levels which permit stronger binding of the compounds within the allosteric site of wtIDH1, and low nutrient levels (e.g., glucose in particular) which increase cancer cell reliance on the wild-type isoenzyme. The presence of these specific conditions render cancer cells vulnerable to allosteric IDH1 inhibition.

In the present study, we sought to build on the prior work to more firmly establish wtIDH1 as a therapeutic target in melanoma and leverage novel insights to propose an immediately translatable therapeutic strategy for patients. In this study, wtIDH1 appeared to be important for melanoma survival under nutrient limited conditions, and genetic ablation of the enzyme slowed tumor growth in mouse melanoma models. Findings observed with IDH1 suppression were phenocopied by AG-120 treatment.

Cytotoxic chemotherapeutics remain the treatment backbone across most tumor types [52–56], yet have been largely abandoned for melanoma. Currently, chemotherapy usage is limited to patients with metastatic melanoma after disease progression or drug intolerance with immunotherapy or oncogene-targeted agents [57]. Moreover, there is little hope for a clinically impactful survival advantage in these scenarios. Cytotoxic treatment options include TMZ (alkylating agent), DTIC (alkylating agent), paclitaxel (or albumin-bound paclitaxel) (microtubule inhibitor), and carboplatin (platinum agent and DNA cross-linker) [58]. The most commonly used among these agents, TMZ (an oral prodrug of DTIC) and DTIC, have roughly equivalent activity against melanoma [59]. Progression-free and overall survivals associated with these agents in patients with advanced melanoma are dismal and frankly unacceptable-just 2 and 7 months, respectively. Less than 20% of patients survive beyond 2 years without the benefit of newer therapies [12]. These results have prompted investigations into mechanisms to induce chemo-sensitization in melanoma as a strategy to offer readily available second or third-line options for patients with refractory disease. A common thread among many of the studies is the use of adjuvants that promote oxidative stress as a mechanism to reduce chemotherapy resistance in melanoma cells [30, 60]. In this study, IDH1 inhibition with AG-120 potently induced oxidative stress in melanoma cells under nutrient limitation (Supplementary Fig. S5C and D), and effectively synergized with conventional anti-melanoma chemotherapy in cell culture and in mouse melanoma models.

Conclusions

IDH1 inhibition profoundly impairs the growth of melanoma cells in culture and xenografts in mice. IDH1 suppression enhances ROS and impairs mitochondrial function in tumors. As a result, wtIDH1 inhibition with AG-120 was effective against melanoma tumors, especially in combination with a conventional anti-melanoma cytotoxic agent (TMZ). Future studies aimed at validating these findings in additional melanoma cancer models will provide an even stronger rationale to test AG-120 (ivosidenib) and chemotherapy in patients with refractory metastatic melanoma. We are currently initiating a prospective phase Ib trial combining ivosidenib and multi-agent chemotherapy in patients with pancreatic cancer (NCT05209074). The present findings also provide a justification for a similar approach in patients with treatment refractory and advanced melanoma.

Abbreviations

IDH1: Isocitrate dehydrogenase 1; TMZ: Temozolomide; ROS: Reactive oxygen species; TCGA: The Cancer Genome Atlas; TCA: Tricarboxylic acid cycle; α-KG: Alpha-Ketoglutarate; GSH: Glutathione.

Supplementary Information

The online version contains supplementary material available at https://doi.org/10.1186/s13046-022-02489-w.

Additional file 1: Supplementary Figure 1. IDH1 promotes cell migration under glucose limitation in melanoma cells. A] and B] Caspase3/7 activity was measured in A375 and SK-MEL-28 cells after 48 hours silencing IDH1 compared to control under low glucose concentration (2.5 mM). C] Representative cell images of A375 (4X magnification) and quantification of transwell migration under the indicated conditions after silencing IDH1 compared to control. D] SK-MEL-28 cell images (4X magnification) and quantitation of transwell migration under the indicated glucose concentrations. Each data point represents the mean ± SEM of at least three independent experiments. N.S., nonsignificant; *, $P < 0.05$; **, $P < 0.01$; ***, $P < 0.001$.

Additional file 2: Supplementary Figure 2. IDH1 supports mitochondrial function under glucose limitation. A] Representative OCR tracing in A375 melanoma cells cultured under the indicated glucose concentrations for 24 hours and B] Extracellular acidification rate (ECAR) response of A375 cells under the indicated conditions. C] PCA of metabolites analyzed by LC-MS/MS performed on A375 cells under high (25 mM) and low (2.5 mM) glucose ($n = 3$ samples). D] A heatmap of the top 50 metabolites with the greatest changes in A375 cells ($n = 3$ independent samples) under 25 mM glucose. The scale is log 2 fold-change. E] Representative OCR tracing in A375 melanoma cells cultured under the indicated glucose concentrations for 24 hours.

Additional file 3: Supplementary Figure 3. AG-120 is a potential wtIDH1 inhibitor under glucose limitation in melanoma cells. A] Representative images of colony formation assays for cells cultured under high (25 mM) and B] low glucose (2.5 mM) in the SK-MEL-28 cell line. The cells were treated with vehicle control or AG-120 (2 μM) under the indicated conditions for 9 days. Quantitation (%) is shown in the graph at the bottom. C] Cells cultured under high glucose, or D] low glucose were captured by phase-contrast imaging (4X magnification), after treatment with vehicle control or AG-120 (2 μM) for 4 days. Representative oxygen consumption rate (OCR) in A375 E] and SK-MEL-28 F] cell lines cultured in 2.5 mM glucose and treated with vehicle or AG-120 for 36 hours. G] and H] Basal mitochondrial respiration, ATP production, and maximal mitochondrial respiration of the A375 and SK-MEL-28 cells treated with vehicle or AG-120 for 36 hours. Each data point represents the mean ± SEM of three independent experiments. N.S., nonsignificant; *, $P < 0.05$; **, $P < 0.01$; ***, $P < 0.001$.

Additional file 4: Supplementary Figure 4. IDH1 knockout suppresses tumor growth in vivo. A] Relative mRNA levels, normalized to mRNA levels of 18S; Western blot analysis of IDH1 expression after IDH1 knockout by CRISPR/Cas9 (IDH1.KO) compared to control (IDH1.EV) A375 cells. B] Mice were injected with IDH1.EV and IDH1.KO A375 cells ($n = 5$ per group) and tumor sizes were monitored for 5 weeks. Images of tumors at the end of the experiment are shown. C] Tumor volumes of IDH1.EV and IDH1.KO A375 xenografts. D] Histograms show tumor volumes with IDH1.EV and IDH1.KO A375 xenografts at the end of the experiment. E] Relative glucose levels in adjacent skin and xenograft. F] Relative free magnesium levels in skin, xenografts and serum. Each data point represents the mean ± SEM. *, $P < 0.05$; **, $P < 0.01$; ***, $P < 0.001$; ****, $P < 0.0001$.

Additional file 5: Supplementary Figure 5. In vitro response of melanoma cells to treatment with TMZ in combination with AG-120. A] Silencing *IDH1* followed by treatment with TMZ for 5 days under high glucose (25 mM) and B] low glucose (2.5 mM) in SK-MEL-28 cells; IC50 values are provided. C] Relative ROS levels after 48 hours in A375 cell line under low glucose combined with TMZ and AG-120. D] Relative ROS levels after 48 hours in SK-MEL-28 cells under low glucose combined with TMZ and AG-120. E] Cell viability of SK-MEL-28 cells, treated with the indicated doses of TMZ; IC50 values are provided. F] Cell viability of SK-MEL-28 cells treated with indicated doses of AG-120 for 6 days. IC50 values are provided. G] Drug sensitivity in SK-MEL-28 cells under low glucose, with varying concentrations of TMZ and AG-120, cultured for 5 days under low glucose. IC50 results are provided. H] Drug matrix heatmap 5 × 8 (AG-120 and TMZ) grid showing percent viability and Bliss Independence scores in SK-MEL-28 cells cultured under 2.5 mM glucose for 5 days. Positive values reflecting synergism appear green on the heatmap (Bliss volume ≥ 10). All treatments with AG-120 were carried under low glucose (2.5 mM) and low Mg2+ (0.08 mM).

Additional file 6: Supplementary Figure 6. Treatment of mice bearing B16-F10 tumors with TMZ in combination with AG-120. A] Sanger sequencing of PCR amplicons correlated with codon 132 of the IDH1 gene in B16-F10 murine melanoma cells. B] Schematic represents the treatment model after 4 × 104 B16-F10 melanoma murine cells were injected subcutaneously into the flanks of C57BL/6 J recipient mice. After 9 days, when tumors reached 80-100 mm3, mice were divided into four groups and treated with i) Vehicle; ii) TMZ (30 mg/kg intraperitoneal once a day); iii) AG-120 (150 mg/kg orally twice a day); and iv) AG-120 + TMZ (150 mg/kg orally twice a day + 30 mg/kg intraperitoneal daily). C] Survival data of C57BL/6 J mice are represented by Kaplan-Meier curves. Significance between each group was determined using the log-rank test.

Acknowledgments
Not applicable.

Authors' contributions
MZ: Investigation, conceptualization, data curation methodology, writing-original draft, writing–review and editing. OH: Investigation, methodology. JJH: Investigation, methodology. HJG: Investigation, methodology. AWL: Investigation, methodology, MR: Investigation, methodology AVG: Investigation, methodology. JMA: Investigation, methodology. JMW: Conceptualization, funding acquisition, supervision, administration, writing and editing. LDR: Conceptualization, funding acquisition, supervision, administration, writing and editing. All authors read and approved the final manuscript.

Funding
Grant support for this research comes the American Cancer Society MRSG-14-019-01-CDD, American Cancer Society 134170-MBG-19-174-01-MBG, NCI R37CA227865-01A1, the Case Comprehensive Cancer Center GI SPORE 5P50CA150964-08, Case Comprehensive Cancer Center core grant P30CA043703, and University Hospitals research start-up package (J.M.W.). We are grateful for additional support from numerous donors to the University Hospitals Surgical Oncology Lab, including the John and Peggy Garson Family Research Fund, The Jerome A. and Joy Weinberger Family research fund, Robin Holmes-Novak in memory of Eugene, and Rosi and Saby Behar.

Availability of data and materials
Not applicable.

Declarations

Ethics approval and consent to participate
Not applicable.

Consent for publication
Not applicable.

Competing interests
J.M.W. along with University Hospitals, filed the following patent application on September 24, 2020: Methods for Treating Wild Type Isocitrate Dehydrogenase 1 Cancers. Information regarding this patent application is as follows: PCT/US20/52445 filed 09/24/20, Claiming Priority to US 62/911,717 filed 10/7/19, File Nos: UHOSP-19738 | 2019-014.

Author details
[1]Case Comprehensive Cancer Center, Case Western Reserve University, Cleveland, OH, USA. [2]Department of Surgery, Division of Surgical Oncology, University Hospitals Cleveland Medical Center, 11100 Euclid Ave., Cleveland, OH 44106, USA. [3]Division of Signal Transduction and Mass Spectrometry Core, Beth Israel Deaconess Medical Center, Boston, MA, USA. [4]Department of Medicine, Harvard Medical School, Boston, MA, USA.

Received: 18 May 2022 Accepted: 6 September 2022
Published online: 24 September 2022

References

1. Grünhagen DJ, Kroon HM, Verhoef C. Perfusion and infusion for melanoma in-transit metastases in the era of effective systemic therapy. Am Soc Clin Oncol Educ B. 2015;35:e528–34 American Society of Clinical Oncology Alexandria, VA.
2. Sullivan RJ, Atkins MB, Kirkwood JM, Agarwala SS, Clark JI, Ernstoff MS, et al. An update on the Society for Immunotherapy of Cancer consensus statement on tumor immunotherapy for the treatment of cutaneous melanoma: version 2.0. J Immunother Cancer. 2018;6:1–23 Springer.
3. Siegel R, Ward E, Brawley O, Jemal A. Cancer statistics, 2011: the impact of eliminating socioeconomic and racial disparities on premature cancer deaths. CA Cancer J Clin. 2011;61:212–36.
4. Wolchok JD, Chiarion-Sileni V, Gonzalez R, Grob J-J, Rutkowski P, Lao CD, et al. CheckMate 067: 6.5-year outcomes in patients (pts) with advanced melanoma. J Clin Oncol. 2021;39:Suppl 15:9506 American Society of Clinical Oncology.
5. Tsao H, Atkins MB, Sober AJ. Management of cutaneous melanoma. N Engl J Med. 2004;351:998–1012 Mass Medical Soc.
6. Larkin J, Chiarion-Sileni V, Gonzalez R, Grob J-J, Rutkowski P, Lao CD, et al. Five-year survival with combined nivolumab and ipilimumab in advanced melanoma. N Engl J Med. 2019;381:1535–46 Mass Medical Soc.
7. Larkin J, Chiarion-Sileni V, Gonzalez R, Grob JJ, Cowey CL, Lao CD, et al. Combined nivolumab and ipilimumab or monotherapy in untreated melanoma. N Engl J Med. 2015;373:23–34 Mass Medical Soc.
8. Gide TN, Wilmott JS, Scolyer RA, Long GV. Primary and acquired resistance to immune checkpoint inhibitors in metastatic melanoma. Clin Cancer Res. 2018;24:1260–70 AACR.
9. Eroglu Z, Ribas A. Combination therapy with BRAF and MEK inhibitors for melanoma: latest evidence and place in therapy. Ther Adv Med Oncol. 2016;8:48–56 SAGE Publications Sage UK: London, England.
10. Long GV, Stroyakovskiy D, Gogas H, Levchenko E, de Braud F, Larkin J, et al. Combined BRAF and MEK inhibition versus BRAF inhibition alone in melanoma. N Engl J Med. 2014;371:1877–88 Mass Medical Soc.
11. Eggermont AMM, Kirkwood JM. Re-evaluating the role of dacarbazine in metastatic melanoma: what have we learned in 30 years? Eur J Cancer. 2004;40:1825–36 Elsevier.
12. Middleton MR, Grob JJ, Aaronson N, Fierlbeck G, Tilgen W, Seiter S, et al. Randomized phase III study of temozolomide versus dacarbazine in the

treatment of patients with advanced metastatic malignant melanoma. J Clin Oncol. 2000;18:158 American Society of Clinical Oncology.
13. Agarwala SS, Kirkwood JM. Temozolomide, a novel alkylating agent with activity in the central nervous system, may improve the treatment of advanced metastatic melanoma. Oncologist. 2000;5:144–51 Oxford University Press.
14. Dratkiewicz E, Simiczyjew A, Mazurkiewicz J, Ziętek M, Matkowski R, Nowak D. Hypoxia and extracellular acidification as drivers of melanoma progression and drug resistance. Cells. 2021;10:862 Multidisciplinary Digital Publishing Institute.
15. Gupta S, Roy A, Dwarakanath BS. Metabolic cooperation and competition in the tumor microenvironment: implications for therapy. Front Oncol. 2017;7:68 Frontiers.
16. Fischer GM, Vashisht Gopal YN, McQuade JL, Peng W, DeBerardinis RJ, Davies MA. Metabolic strategies of melanoma cells: mechanisms, interactions with the tumor microenvironment, and therapeutic implications. Pigment Cell Melanoma Res. 2018;31:11–30 Wiley Online Library.
17. Jose C, Bellance N, Rossignol R. Choosing between glycolysis and oxidative phosphorylation: a tumor's dilemma? Biochim Biophys Acta. 2011;1807:552–61 Elsevier.
18. Birsoy K, Possemato R, Lorbeer FK, Bayraktar EC, Thiru P, Yucel B, et al. Metabolic determinants of cancer cell sensitivity to glucose limitation and biguanides. Nature. 2014;508:108–12 Nature Publishing Group.
19. Rossignol R, Gilkerson R, Aggeler R, Yamagata K, Remington SJ, Capaldi RA. Energy substrate modulates mitochondrial structure and oxidative capacity in cancer cells. Cancer Res. 2004;64:985–93 AACR.
20. Zarei M, Lal S, Parker SJ, Nevler A, Vaziri-Gohar A, Dukleska K, et al. Post-transcriptional upregulation of IDH1 by HuR establishes a powerful survival phenotype in pancreatic cancer cells. Cancer Res. 2017;77:4460–71 AACR.
21. Jiang L, Shestov AA, Swain P, Yang C, Parker SJ, Wang QA, et al. Reductive carboxylation supports redox homeostasis during anchorage-independent growth. Nature. 2016;532:255–8 Nature Publishing Group.
22. Mullen AR, Wheaton WW, Jin ES, Chen P-H, Sullivan LB, Cheng T, et al. Reductive carboxylation supports growth in tumour cells with defective mitochondria. Nature. 2012;481:385–8 Nature Publishing Group.
23. Metallo CM, Gameiro PA, Bell EL, Mattaini KR, Yang J, Hiller K, et al. Reductive glutamine metabolism by IDH1 mediates lipogenesis under hypoxia. Nature. 2012;481:380–4 Nature Publishing Group.
24. Vaziri-Gohar A, Cassel J, Mohammed FS, Zarei M, Hue JJ, Hajihassani O, et al. Limited nutrient availability in the tumor microenvironment renders pancreatic tumors sensitive to allosteric IDH1 inhibitors. Nat Cancer. 2022;3:852-856 Nature Publishing Group.
25. Jakob CG, Upadhyay AK, Donner PL, Nicholl E, Addo SN, Qiu W, et al. Novel modes of inhibition of wild-type isocitrate dehydrogenase 1 (IDH1): direct covalent modification of His315. J Med Chem. 2018;61:6647–57 ACS Publications.
26. Okoye-Okafor UC, Bartholdy B, Cartier J, Gao EN, Pietrak B, Rendina AR, et al. New IDH1 mutant inhibitors for treatment of acute myeloid leukemia. Nat Chem Biol. 2015;11:878–86 Nature Publishing Group.
27. Urban DJ, Martinez NJ, Davis MI, Brimacombe KR, Cheff DM, Lee TD, et al. Assessing inhibitors of mutant isocitrate dehydrogenase using a suite of pre-clinical discovery assays. Sci Rep. 2017;7:1–15 Nature Publishing Group.
28. Zarei M, Hue JJ, Hajihassani O, Graor HJ, Katayama ES, Loftus AW, et al. Clinical development of IDH1 inhibitors for cancer therapy. Cancer Treat Rev. 2021;103:102334 Elsevier.
29. Seltzer MH, Rosato FE, Fletcher MJ. Serum and tissue magnesium levels in human breast carcinoma. J Surg Res. 1970;10:159–62 Elsevier.
30. Tse AK-W, Chen Y-J, Fu X-Q, Su T, Li T, Guo H, et al. Sensitization of melanoma cells to alkylating agent-induced DNA damage and cell death via orchestrating oxidative stress and IKKβ inhibition. Redox Biol. 2017;11:562–76 Elsevier.
31. Liu Q, Yin X, Languino LR, Altieri DC. Evaluation of drug combination effect using a bliss independence dose–response surface model. Stat Biopharm Res. 2018;10:112–22 Taylor & Francis.
32. Ziebart T, Walenta S, Kunkel M, Reichert TE, Wagner W, Mueller-Klieser W. Metabolic and proteomic differentials in head and neck squamous cell carcinomas and normal gingival tissue. J Cancer Res Clin Oncol. 2011;137:193–9 Springer.
33. Peltz C, Schroeder T, Dewhirst MW. Monitoring metabolite gradients in the blood, liver, and tumor after induced hyperglycemia in rats with R3230 flank tumors using microdialysis and bioluminescence imaging. Adv Exp Med Biol 2005;566:343–8.
34. Kamphorst JJ, Nofal M, Commisso C, Hackett SR, Lu W, Grabocka E, et al. Human pancreatic cancer tumors are nutrient poor and tumor cells actively scavenge extracellular protein. Cancer Res. 2015;75:544–53 AACR.
35. Nardo G, Favaro E, Curtarello M, Moserle L, Zulato E, Persano L, et al. Glycolytic phenotype and AMP kinase modify the pathologic response of tumor xenografts to VEGF neutralization. Cancer Res. 2011;71:4214–25 AACR.
36. Taylor NJ, Gaynanova I, Eschrich SA, Welsh EA, Garrett TJ, Beecher C, et al. Metabolomics of primary cutaneous melanoma and matched adjacent extratumoral microenvironment. PLoS One. 2020;15:e0240849 Public Library of Science San Francisco, CA USA.
37. Zarei M, Shrestha R, Johnson S, Yu Z, Karki K, Vaziri-Gohar A, et al. Nuclear receptor 4A2 (NR4A2/NURR1) regulates autophagy and chemoresistance in pancreatic ductal adenocarcinoma. Cancer Res Commun. 2021;1:65–78 AACR.
38. Yuan M, Breitkopf SB, Yang X, Asara JM. A positive/negative ion–switching, targeted mass spectrometry–based metabolomics platform for bodily fluids, cells, and fresh and fixed tissue. Nat Protoc. 2012;7:872–81 Nature Publishing Group.
39. DiNardo CD, Stein EM, de Botton S, Roboz GJ, Altman JK, Mims AS, et al. Durable remissions with ivosidenib in IDH1-mutated relapsed or refractory AML. N Engl J Med. 2018;378:2386–98 Mass Medical Soc.
40. Abou-Alfa GK, Macarulla T, Javle MM, Kelley RK, Lubner SJ, Adeva J, et al. Ivosidenib in IDH1-mutant, chemotherapy-refractory cholangiocarcinoma (ClarIDHy): a multicentre, randomised, double-blind, placebo-controlled, phase 3 study. Lancet Oncol. 2020;21:796–807 Elsevier.
41. Mellinghoff IK, Ellingson BM, Touat M, Maher E, De La Fuente MI, Holdhoff M, et al. Ivosidenib in isocitrate dehydrogenase 1–mutated advanced glioma. J Clin Oncol. 2020;38:3398 American Society of Clinical Oncology.
42. Nicolay B, Narayanaswamy R, Aguado E, Nagaraja R, Murtie J, Liu G, et al. The IDH1 mutant inhibitor AG-120 shows strong inhibition of 2-HG production in an orthotopic IDH1 mutant glioma model in vivo. Neuro Oncol. 2017;19:vi86.
43. Popovici-Muller J, Lemieux RM, Artin E, Saunders JO, Salituro FG, Travins J, et al. Discovery of AG-120 (Ivosidenib): a first-in-class mutant IDH1 inhibitor for the treatment of IDH1 mutant cancers. ACS Med Chem Lett. 2018;9:300–5 ACS Publications.
44. Kaufmann R, Spieth K, Leiter U, Mauch C, von den Driesch P, Vogt T, et al. Temozolomide in combination with interferon-alfa versus temozolomide alone in patients with advanced metastatic melanoma: a randomized, phase III, multicenter study from the Dermatologic Cooperative Oncology Group. J Clin Oncol. 2005;23:9001–7 American Society of Clinical Oncology.
45. Le Gal K, Ibrahim MX, Wiel C, Sayin VI, Akula MK, Karlsson C, et al. Antioxidants can increase melanoma metastasis in mice. Sci Transl Med. 2015;7:308re8 American Association for the Advancement of Science.
46. Sayin VI, Ibrahim MX, Larsson E, Nilsson JA, Lindahl P, Bergo MO. Antioxidants accelerate lung cancer progression in mice. Sci Transl Med. 2014;6:221ra15 American Association for the Advancement of Science.
47. Group A-TBCCPS. The effect of vitamin E and beta carotene on the incidence of lung cancer and other cancers in male smokers. N Engl J Med. 1994;330:1029–35 Mass Medical Soc.
48. Klein EA, Thompson IM, Tangen CM, Crowley JJ, Lucia MS, Goodman PJ, et al. Vitamin E and the risk of prostate cancer: the Selenium and Vitamin E Cancer Prevention Trial (SELECT). JAMA. 2011;306:1549–56 American Medical Association.
49. Perillo B, Di Donato M, Pezone A, Di Zazzo E, Giovannelli P, Galasso G, et al. ROS in cancer therapy: the bright side of the moon. Exp Mol Med. 2020;52:192–203 Nature Publishing Group.
50. Piskounova E, Agathocleous M, Murphy MM, Hu Z, Huddlestun SE, Zhao Z, et al. Oxidative stress inhibits distant metastasis by human melanoma cells. Nature. 2015;527:186–91 Nature Publishing Group.
51. Calvert AE, Chalastanis A, Wu Y, Hurley LA, Kouri FM, Bi Y, et al. Cancer-associated IDH1 promotes growth and resistance to targeted therapies in the absence of mutation. Cell Rep. 2017;19:1858–73.

52. Bikov KA, Mullins CD, Seal B, Onukwugha E, Hanna N. Algorithm for identifying chemotherapy/biological regimens for metastatic colon cancer in SEER-Medicare. Med Care. 2015;53:e58–64 JSTOR.
53. Balkhi B, Alqahtani S, Altayyar W, Ghawaa Y, Alqahtani Z, Alsaleh K, et al. Drug utilization and expenditure of anticancer drugs for breast cancer. Saudi Pharm J. 2020;28:669–74 Elsevier.
54. Gau M, Karabajakian A, Reverdy T, Neidhardt E-M, Fayette J. Induction chemotherapy in head and neck cancers: results and controversies. Oral Oncol. 2019;95:164–9 Elsevier.
55. Chen X, Zeh HJ, Kang R, Kroemer G, Tang D. Cell death in pancreatic cancer: from pathogenesis to therapy. Nat Rev Gastroenterol Hepatol. 2021;18:804–23 Nature Publishing Group.
56. El-Hussein A, Manoto SL, Ombinda-Lemboumba S, Alrowaili ZA, Mthunzi-Kufa P. A review of chemotherapy and photodynamic therapy for lung cancer treatment. Anti-Cancer Agents Med Chem (Formerly Curr Med Chem Agents). 2021;21:149–61 Bentham Science Publishers.
57. Coit DG, Thompson JA, Albertini MR, Barker C, Carson WE, Contreras C, et al. Cutaneous melanoma, version 2.2019, NCCN clinical practice guidelines in oncology. J Natl Compr Cancer Netw. 2019;17:367–402 National Comprehensive Cancer Network.
58. Schmults CD, Blitzblau R, Aasi SZ, Alam M, Andersen JS, Baumann BC, et al. NCCN guidelines® insights: squamous cell skin cancer, version 1.2022: featured updates to the NCCN guidelines. J Natl Compr Cancer Netw. 2021;19:1382–94 National Comprehensive Cancer Network.
59. Quirt I, Verma S, Petrella T, Bak K, Charette M. Temozolomide for the treatment of metastatic melanoma: a systematic review. Oncologist. 2007;12:1114–23 Oxford University Press.
60. Campagna R, Bacchetti T, Salvolini E, Pozzi V, Molinelli E, Brisigotti V, et al. Paraoxonase-2 silencing enhances sensitivity of A375 melanoma cells to treatment with cisplatin. Antioxidants. 2020;9:1238 Multidisciplinary Digital Publishing Institute.

Publisher's Note